FOREX Publication
Open Access | Rapid and quality publishing

International Journal of
Electrical and Electronics Research (IJEER)
Research Article | Volume 11, Issue 2 | Pages 478-484 | e-ISSN: 2347-470X

Power Circuit Design and Analysis of Controller for High-Power Axial Flux PMSM

T. Neelakanteswara Reddy[1], Gautam Monipatro[2] and P. Mallikarjuna Rao[3]

[1]Research Scholar, Dept. of Electrical Engineering, Andhra University, Visakhapatnam, India., eswar.eee19@gmail.com
[2]Senior Research Fellow, Dept. of Electrical Engineering, Andhra University, Visakhapatnam, India., gautammp@yahoo.co.in
[3]Professor, Dept. of Electrical Engineering, Andhra University, Visakhapatnam, India., electricalprofessor@gmail.com

***Correspondence:** T. Neelakanteswara Reddy; eswar.eee19@gmail.com; Tel.: +91-9533770143

ABSTRACT- Designing a high-power controller having high efficiency for permanent magnet motors is a challenge for developers in recent times and very few techniques are available. Design and analysis of power electronic drive for a high-power axial flux permanent magnet synchronous motor is presented in this paper. The motor under consideration here is having two outer stators and single permanent magnet rotor to drive the shaft. Control schemes and methodologies are the major concentration for research. Present paper explains a method to estimate the operational drive parameters and loss calculation according the selected power switches. In addition to this, thermal modelling is also important for designing a controller for high power machines. The hardware selection for high current switching operations is very critical for reliable and robust operation. Parts like IGBT module, gate driver, DC link capacitor, snubbers, current sensor sensitivities and estimation of losses are also critical along with control logic and processor. The importance of thermal analysis for high current switching drives is discussed and methodology for thermal analysis of power electronic devices is explained. The current work focuses on hardware level design of high-power drive for 150kW axial flux PMS motor.

Keywords: Power Electronic Drive, AFPMSM, IGBT, filter capacitors, motor simulations

ARTICLE INFORMATION

Author(s): T. Neelakanteswara Reddy, Gautam Monipatro and P. Mallikarjuna Rao;

Received: 15/04/2023; **Accepted**: 29/05/2023; **Published:** 30/06/2023;
E- ISSN: 2347-470X;
Paper Id: IJEER230407;
Citation: 10.37391/IJEER.110231
Webpage-link:
https://ijeer.forexjournal.co.in/archive/volume-11/ijeer-110231.html

Publisher's Note: FOREX Publication stays neutral with regard to Jurisdictional claims in Published maps and institutional affiliations.

1. INTRODUCTION

In recent era, demand of high-power axial flux permanent magnet machine drives increased in view of industrial and scientific applications [1]. These machines have high power density, better magnetic and electrical loading capacity, long life and low noise [2].

For the power electronic drive, important requirement is component selection suitable for high current switching and minimizing losses. For the current application, SVPWM [3] control algorithms are implemented in the DSC and a master processor commands the DSC. ARM CORTEX M4 based architecture is adopted for the Master Processor. The space vector modulation and closed loop vector control algorithms are implemented in the DSC. IGBTs are selected for rated current and voltage requirements with necessary factor of safety. Numerous literatures [4] are available for control logics and techniques Axial Flux PMS motor [5]. In view of practical implementation care has to be taken for high current and high frequency switching.

The IGBTs will share the phase current by parallel operation. The parallel operation is opted for optimization of losses and description of heat. DC link capacitors, snubber capacitors, bus bars, DC-DC converters, sensors, processors, driver boards and power terminals are selected and accommodated in a best possible layout in order to optimize the space and weight of the overall power electronic drive system.

Table 1. List of vital input design specifications

Parameter	Value
Input voltage	360V DC minimum up to 550V OCV
Input source	Battery
Type of power devices	IGBT
Nature of the Load	Axial Flux PMSM Motor
Speed of the Motor	1800 RPM per Motor at full load
Output power	163 kW
Output voltage variation	0 to 100% & 100% to 0 by space vector PWM
Efficiency	96-97%
Controller Strategy	PMSM vector control with communication
Acceleration time	08 sec from rest to rated 1800rpm speed on load
Rotor position sensing	360V DC minimum up to 550V OCV

The estimation of operational drive parameters like winding currents, switching frequency and also taking current ripple into account. The hardware selection for high current switching operations is very critical for reliable and robust operation. Parts

FOREX Publication
Open Access | Rapid and quality publishing
International Journal of Electrical and Electronics Research (IJEER)
Research Article | Volume 11, Issue 2 | Pages 478-484 | e-ISSN: 2347-470X

like IGBT module, gate driver, DC link capacitor, snubbers, current sensor sensitivities and estimation of losses [6] are also critical along with control logic [7-8] and processor.

After an extensive study and search for the literature in this regard, it is observed there is a very minimal literature available for hardware level design. So, data from different developers and manufactures is collected and efforts put on presenting an elaborate methodology to estimate the specifications of the required hardware for the drive design.

Table 2. List of critical derived input design parameters

Parameter	Value
Input power	150kW
Input current	500A DC
Max Modulation Index	0.9 (Assumed)
Output power	158KW
IGBT Switching Frequency	10 kHz
Ambient temperature	30° C
Max allowable Heat-sink Temperature	85° C
Max allowable junction temperature of IGBT	150° C
Max allowable capacitor Temperature	85° C

Table 2 shows the important parameters that are derived from the motor to design the dive hardware. Few limitations related to thermal management, run time error and processing speed (Switching speed) have been eliminated with this new methodology.

The following section explains clearly the design methodology, selection of power circuit hardware and simulations to estimate the functionality of the designed power electronic drive for 150kW axial flux PMS motor using simulations. Thermal analysis is also done using lumped parameter model to ensure safe operation at high current switching.

2. DESIGN METHADOLOGYTY

Figure 1 shows the power circuit schematic for the 165kW power electronic drive system. The total controller has inverter to drive the 150kW axial flux PMS motor. As can be seen from the figure, the DC battery drives the inverter. The DC voltage is applied to the drive through a high-power contactor. The three-phase inverter bridge of each motor are driven by respective adapter and gate driver boards.

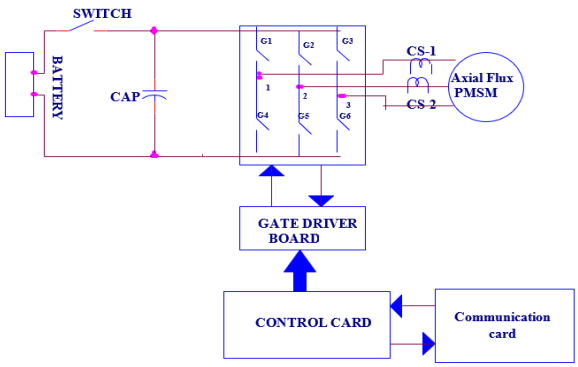

Figure 1: Circuit schematic of the power electronic drive

The vector control logic is implemented in the control board with one common digital signal controller. This processor on the control board acts like slave and are commanded by the master processor on the communication card. The control takes the necessary phase current and rotor position inputs from respective motors and with the help of vector control logic [9] generates the PWM signals for the gates of IGBT based inverters. The input DC link capacitors will help in maintaining the minimum current ripples on the DC bus of the system. The control card also implements the necessary protection logics for the motor drives.

The 150kW axial flux motor is designed with two stator cores. The motor will be made of two 75kW stator cores operating in parallel and driving the same shaft. Both the stator cores are similar to each other. Table 3 shows the parameters required to design a drive for 150kW motor.

Table 3. List of important motor parameters

Parameter	Value
Motor shaft power	150KW
Motor Terminal RMS line voltage	228V
Motor rated speed	1800 RPM
No. of poles	22
Frequency	330Hz
Inductance/phase	0.126 milli-H
Resistance/phase	14.5 milli-Ohms
Power factor	0.9
Motor efficiency	95%

Calculated Input DC Current = 163K/360 = 453A
With modulation index Ma = 1
Maximum output AC voltage (phase peak) of Inverter-1
= Ma * (VDC/2) * 1.15
= 207V

The factor 1.15 is because of the 15% extra voltage achieved by the third harmonic voltage injection in space vector PWM technique.

The required input terminal AC voltage (phase peak) of the motor as per motor design parameters is 186 V.

Operating Modulation Index M_a = 186/207 = 0.9 Output AC voltage (peak) of Inverter = 186*√3 = 322V

Output AC voltage (RMS) of Inverter = 322/√2 = 227.8V

Input Current for Motor (line R.M.S) = 453A

Output Current of Inverter (line Peak) = 453 * √2 = 640A

Capacitor ripple current =$\Delta I_{cap\ RIPPLE}$

$= I_{out\ L\text{-}L\ r.m.s} * sqrt[2M_a\{\sqrt{3}/\Delta 4\Pi + \cos^2\Phi(\sqrt{3}/\Pi - ((9/16)M_a))\}]$

= 240A

Table 4 lists the important power circuit calculations in connection with the power electronic drive. Having derived the basic power circuit parameters, in the following sections all the important components of the drive are designed and analyzed for their performance and suitability.

FOREX Publication
Open Access | Rapid and quality publishing
International Journal of Electrical and Electronics Research (IJEER)
Research Article | Volume 11, Issue 2 | Pages 478-484 | e-ISSN: 2347-470X

Table 4. List of important motor parameters

Parameter	Value	Remarks
Output power of Inverter	158kw	@95% Motor efficiency
Input power to the inverter	163kW	@97% PED efficiency
Input DC current from Battery	455A	@360 DC bus voltage
Maximum available phase voltage peak	186V	With SVPWM
Designed MI	0.9	-
Output AC voltage to each Inverter	228V	RMS
Motor power factor	0.9	-
Output current of Inverter	455A	RMS
Peak value of inverter output current	640A	-

3. POWER ELECTRONIC SWITCHES AND SUITABILITY ANALYSIS

Figure 2 shows the IGBT selected for the controller. As per the design, three IGBT modules will make total drive. Each of the IGBT is a HEX pack having six power semiconductor switches in it. Three IGBTs will make an inverter driving one motor. The top three switches and bottom three switches of the HEX pack IGBT operate in parallel. This means each of the HEX pack IGBT makes one leg of the inverter.

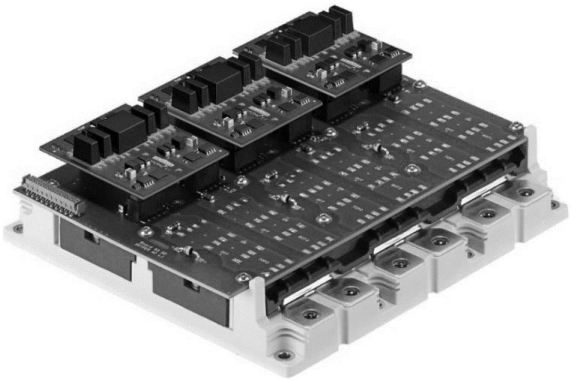

Figure 2: Selected IGBT for the Power Electronic Drive (SKiM306GD12E4)

From the calculated values in previous section, the minimum current and voltage rating of the IGBT required is as follows.

The Minimum current Rating of IGBT = 640 A (Peak)
Minimum voltage Rating of the IGBT= 600 V (OCV)

IGBT should operate without failure in transient conditions also. For this we have considered some scaling factor based on the calculated values in the previous section. The IGBT shown in *figure 2* is 300A and 1200V IGBT with HEX pack configuration [8].

Current Rating of IGBT = 900 A
Scaling factor for current overshoot capability = 1.4
Voltage rating of the IGBT = 1200 V
Scaling factor for voltage capability = 2

Table 5 shows the important gate circuit parameters designed for the power electronic drive. *Figure 3* shows the SKYPER42LJR [9] gate driver selected for the purpose. Since the peak gate current is 20A, for a parallel operation of HEX pack device where in three IGBT switches are to be turned ON/OFF simultaneously, each of the IGBT gate channel can take a maximum of 6.66A only. Accordingly, the ON gate resistance (R_{GON}) and off gate resistance (R_{GOFF}) are calculated as follows.

Minimum Gate Resistance of IGBT = 15-(-8) / 6.66
= 3.453Ω
External Gate Resistance of IGBT = 3.453 – 1.7
= 1.753 Ω
Selected gate resistance = 2 Ω

The peak gate current of each switch for selected gate resistance
= 15-(-8) / 3.7
= 6.21A

The above calculations show that, with selected gate resistances, SKYPER 42LJR can drive the HEX pack IGBT (operating its top three and bottom three switches in parallel). The driver can provide the required peak current, average gate current for the selected PWM frequency of switching.

4. INVERTER LOSS CALCULATION

Table 5 shows the important parameters in connection with the loss calculation of the power electronic drive.

Table 5. Important parameters for loss calculation

Parameter	Value	Remarks
On-state voltage of IGBT, Vceo	0.8V	Datasheet
On-state bulk resistance, Rce	5.5 mΩ	Datasheet
On-state voltage of diode, Vfo	1.1V	Datasheet
Turn-on energy loss/pulse	19mJ	-
Turn-off energy loss/pulse	39mJ	-
Reverse recovery energy loss/pulse	21mJ	-
Collector-Emitter reference voltage	600V	-
Collector reference current	300A	-
Maximum allowed junction temperature	150C	-
DC bus voltage	360V	-
Line to line current peak /switch	210A	Three parallel
Efficiency of the inverter	97.2%	Worst case
Junction to sink thermal resistance (IGBT)	0.116 k/W	Datasheet
Junction to sink thermal resistance diode	0.218 k/W	Datasheet

Table 6 lists the losses of the inverter for the controller by using the different values related to switching and conduction losses [10]. The temperature dependent parameters are also considered.

As the selected gate external resistance is 2 ohms, the parameters dependent on this are reconsidered from the IGBT datasheet respective graphs.

E_{ON} = $28*10^{-3}$ (Joules)
E_{OFF} = $39*10^{-3}$ (Joules)
E_{RR} = $19*10^{-3}$ (Joules)

FOREX Publication
Open Access | Rapid and quality publishing
International Journal of Electrical and Electronics Research (IJEER)
Research Article | Volume 11, Issue 2 | Pages 478-484 | e-ISSN: 2347-470X

Table 6. Calculated losses of the inverter

Parameter	Value	Remarks
IGBT conduction loss	100.66	W
IGBT switching loss	75.68	W
Total IGBT loss	176.348	W
Diode conduction loss	35.43	W
Diode switching loss	46.09	W
Total Diode loss	81.535	W
Total Module loss	1547.3	W
Total Inverter loss	4641.9	W

5. CONTROLLER DESIGN AND PERFORMANCE ANALYSIS

The 150kW axial flux motor with 02 stators (each 75kW) and two central rotors has to be controlled by a single inverter. Inverter controls the parallel of two stators along with one central permanent magnet rotor. The controller uses PID control technique [11] to drive the motor. In order to achieve a smooth and stable motor control performance, gains of various loops play crucial role. These gains are designed using Ziegler & Nichole's [12] method and are fine-tuned by simulation. Also, a ramp command is applied for the speed reference at the rate of 1800RPM for 8 seconds. *Table 7* shows the selected control parameters. The designed motor control and its performance for various speeds and loads has been validated using simulation studies in SIMULINK.

Table 7. Selected control parameters

Parameter	Value
Speed Controller proportional Gain	1
Speed Controller Integral gain	2
Speed Controller Max Limit	135.00%
Speed Controller Min Limit	-10.00%
Current Controller proportional Gain	0.136
Current Controller Integral gain	16
Current Controller Max Limit	100.00%
Current Controller Min Limit	-10.00%
Speed base	1800RPM
Voltage base	400V
Current base	848.4A

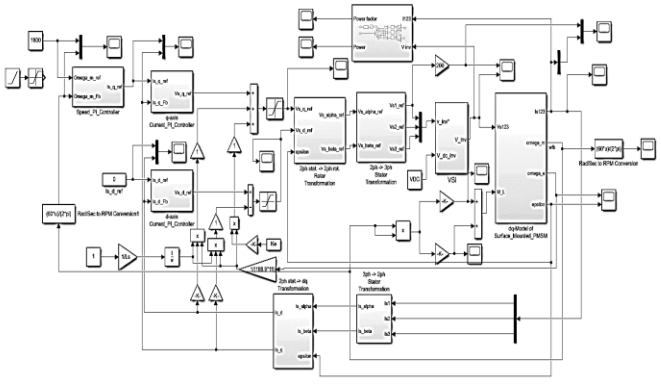

Figure 3: Simulation block for motor and controller

Figure 3 shows the simulation block for the purpose of analysis. *Figure 4* is the speed and current controller subsystems and *figure 5* shows the equivalent PMSM motor model.

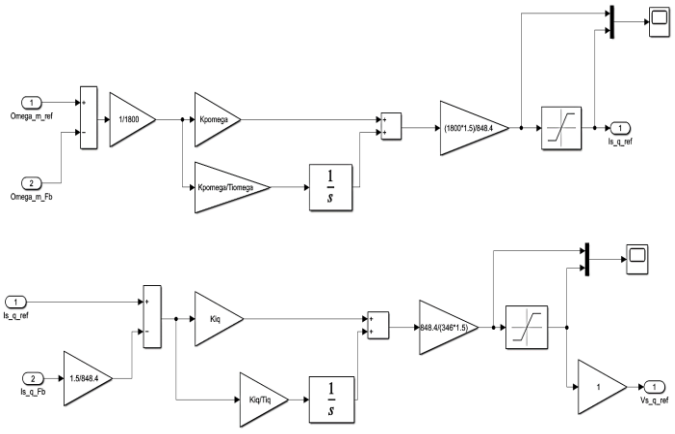

Figure 4: Implemented speed and current controller blocks

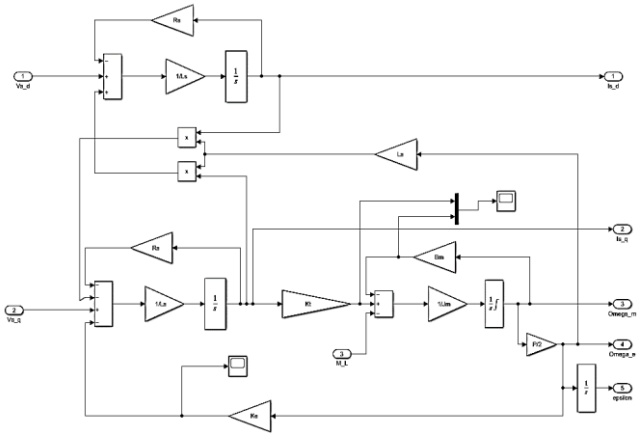

Figure 5: Implemented AF-PMSM motor model

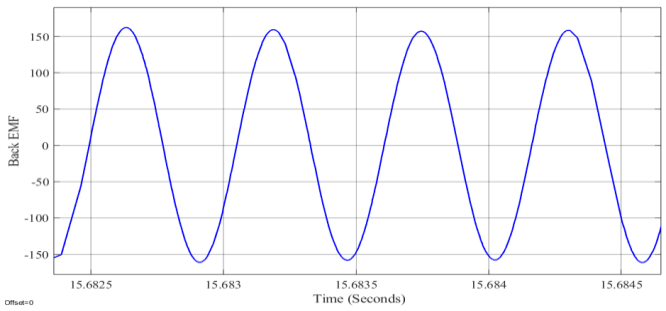

Figure 6: Induced Back EMF per phase @1800rpm

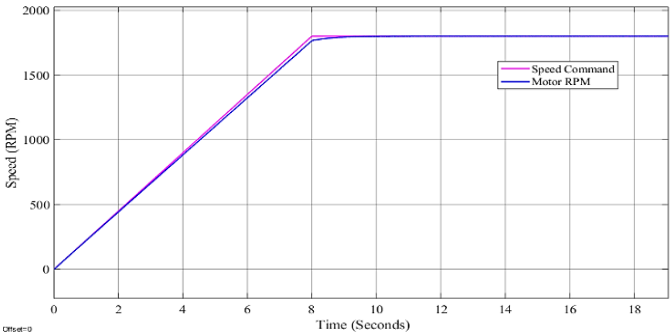

Figure 7: Reference speed command versus rotor speed

FOREX Publication
Open Access | Rapid and quality publishing
International Journal of Electrical and Electronics Research (IJEER)
Research Article | Volume 11, Issue 2 | Pages 478-484 | e-ISSN: 2347-470X

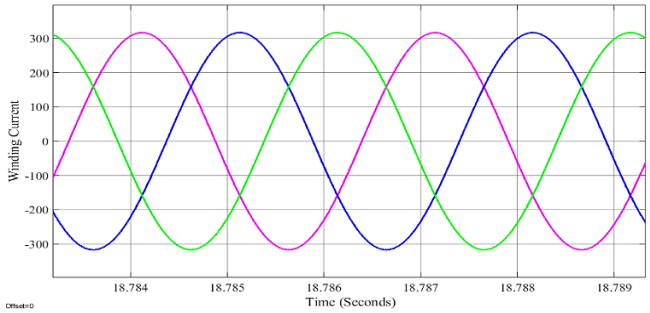

Figure 8: Motor winding currents @ 1800rpm

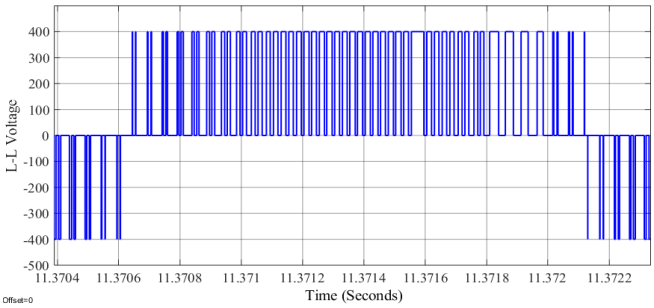

Figure 9: Motor line voltage @ 1800rpm

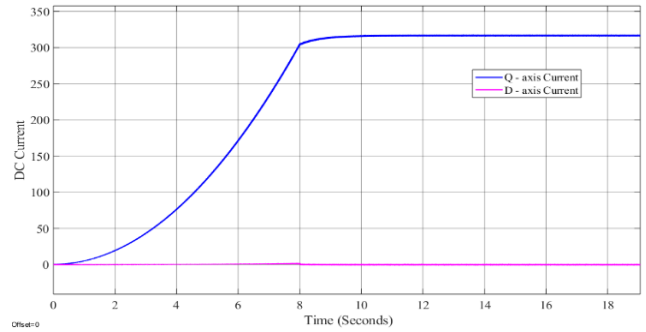

Figure 10: Q-axis and D-axis current @ 1800rpm

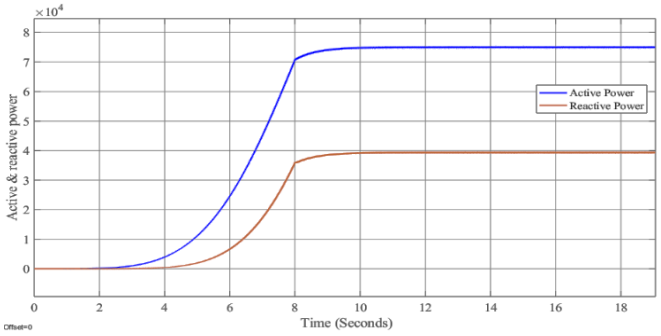

Figure 11: Active and Reactive power @ 1800rpm

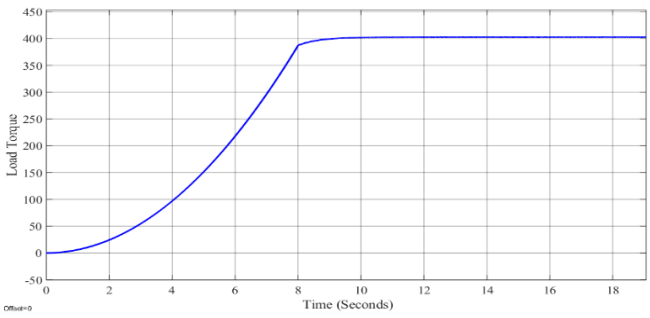

Figure 12: Load Torque/Shaft Torque @ 1800rpm

Figure 6 to figure 12 shows the various important electro-mechanical parameters viz. back EMF, speed response, AC winding currents and voltages, D-Q currents, Active and reactive power and load torque of the for 150kW motor with given reference speed as a ramp of zero to rated *i.e.*, 1800rpm in 8 seconds.

6. THERMAL ANALYSIS

The IGBTs are mounted on the controller box (al alloy). The drive heat sink has cooling channels on the outer periphery which circulates the water at 20 litres/minute in order to take away the heat generated in the IGBTs.

The heat losses generated at the IGBT junctions will transfer to its sink and to the drive shell and to the cooling liquid. Also, some amount of heat will be dissipated through convection and radiation process.

Thermal analysis [10] of 165kW power electronic drive is presented in this section considering these heat transfer aspects. Radiation heat transfer coefficient [11] has been derived.

$$H_r = \sigma * \varepsilon * F_{12} \left[\frac{t_1^4 - t_2^4}{t_1 - t_2}\right]$$

t_1 - Temperatures of the surface
t_2 - Temperature of ambiance
σ - $5.669 \times 10^{-8}\ W/m^2 K^4$
ε - Emissivity (0.7 to 1, 0.8 in present case)
F_{12} - View factor (1 for dissipating surface, 2 for absorbing surface)
H_r - Radiation heat transfer coefficient
R_r - Radiation thermal resistance
A - Radiating surface area

$$R = \frac{1}{H_r * A}$$

Following are a few important correlations for natural convection for a horizontal cylinder.

$$N_{ud} = 0.525 * (Grd * Pr)^{0.25}$$

(For laminar flow when $10^4 < Grd * Pr < 10^9$)

$$N_{ud} = 0.129 * (Grd * Pr)^{0.33}$$

(For turbulent flow when $10^9 < Grd * Pr < 10^{14}$)

$$Grd = \frac{g * \beta * \Delta T * L^3}{v^2}$$

Pr - Pr and tl number
Grd - Grash of number
G - Acceleration due to gravity
B - Thermal expansion coefficient of the fluid
ΔT - Temperature difference between fluid and the surface
L - Characteristic length
v - Kinematic viscosity of the fluid
K - Thermal conductivity of the fluid

$$h_{nc} = \frac{N_{ud} * K}{L}$$

Estimation of the heat transfer coefficient and corresponding thermal resistance is presented in this section.

FOREX Publication
Open Access | Rapid and quality publishing
International Journal of Electrical and Electronics Research (IJEER)
Research Article | Volume 11, Issue 2 | Pages 478-484 | e-ISSN: 2347-470X

Fluid velocity = fluid flow rate (m^3/sec)/flow cross section area,

$$D_h = \frac{4A}{P}$$

$$R_e = \frac{\vartheta D_h}{v}$$

A	-	Area of cross section of the pipe
P	-	Wetted perimeter of the pipe
v	-	Kinematic viscosity of the fluid
D_h	-	Characteristic length
ϑ	-	Velocity of the fluid

And friction factor is

$$f = [0.79 * \ln(R_e) - 1.64]^{-2}$$

$$N_{u0} = \frac{\frac{f}{8}(R_e - 1000) * P_r}{\left[1 + \left(12.7 * \left(\frac{f}{8}\right)^{0.5} * p_r^{\frac{2}{3}} - 1\right)\right]}$$

$$N_{ud} = N_{u0}\left(\frac{\mu_b}{\mu_w}\right)^{0.25}$$

(For the case of fluid in the pipe is being cooled down) which is the present scenario

$$h_c = \frac{N_{ud} * K}{D_h}$$

$$R_t = \frac{1}{h_c * A_s}$$

μ_b - Dynamic viscosity of the fluid at bulk temperature
μ_w - Dynamic viscosity of the fluid at wall temperature
K - Thermal conductivity of the fluid
R_t - Thermal resistance

In the lumped parameter thermal circuit parameters are calculated by the resistance given in the datasheet [8]. The thermal resistance for one IGBT junction to the casing is given. But in the present case we have 3 IGBT modules for controlling single 150(2*75) KW motor. So, coming to the number of junctions we have 6 switches in a single IGBT module and 3 modules which results in total 3*6=18 junctions for a controller. Hence the resultant thermal resistance network is 18 resistances connected in parallel between the sink and controller. *Fig 13* shows the lumped parameter equivalent thermal network for controller thermal analysis.

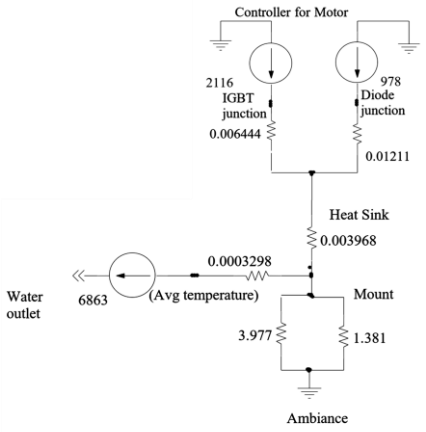

Figure 13: Lumped parameter thermal network for controller forced cooling

Hence, we know when N symmetric resistances are connected in parallel resultant resistance is 1/N times and the current source (losses in transistor) is multiplied by N. As given in the data sheet thermal resistance from junction of single IGBT to sink ($R_{th(j\text{-}s)\ tr}$) = 0.116. In the lumped parameter circuit, the resistance represented is the total resistance due to 18 resistances in the controller is 0.116/18=0.006444C/W. And the current source is the total losses due to the 18 IGBT (switching and conduction losses) is 18* 155.141=2782.51W. similarly, In the anti-parallel diode as given in the data sheet thermal resistance from junction of single diode to sink ($R_{th(j\text{-}s)\ d}$) = 0.218C/W.

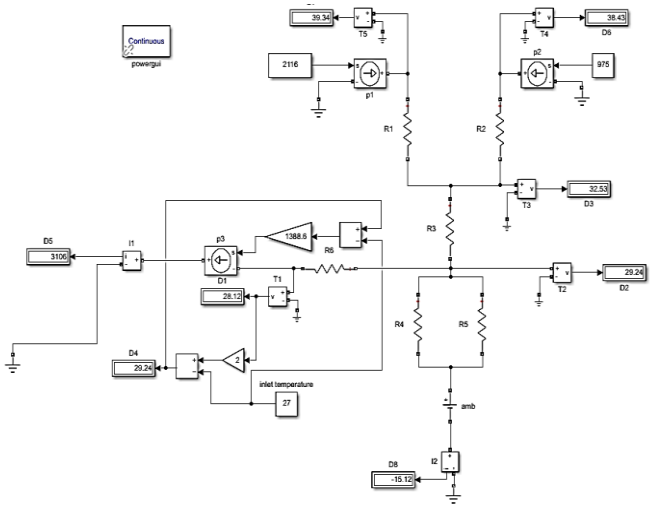

Figure 14: Lumped parameter thermal network for controller forced cooling (simulation)

In the lumped parameter circuit, the resistance represented is the total resistance due to 18 resistances in the controller is 0.218/18=0.01211/W. And the current source for the total losses due to the 18 diodes (switching and conduction losses) is 18*65.545=1179.81W. *Table 8* lists the thermal resistance parameters corresponding this lumped parameter thermal network which was shown in *figure 13*. *Figure 14* presents the Simulink simulation of the external cooling thermal analysis.

Table 8. Calculated node temperatures of controller

Node	Temperature (^{0}C)
Water inlet temperature	27
Water average temperature	29.86
Water outlet temperature	32.72
Temperature at IGBT Junction	82
Temperature at Diode junction	78.3

7. CONCLUSION & FUTURE SCOPE

Power circuit for a high-power drive with high efficiency for a 150kW permanent magnet synchronous motor is designed and methodology is clearly explained. The motor considered here is a state-of-the-art motor configuration having two outer stators and single permanent magnet rotor to drive the shaft. Operational drive parameters like DC bus voltage, winding currents, switching frequency and also taking current ripple

International Journal of
Electrical and Electronics Research (IJEER)
Research Article | Volume 11, Issue 2 | Pages 478-484 | e-ISSN: 2347-470X

currents are calculated and suitable hardware specifications are derived. Critical parts selection such as IGBT module, gate drive and loss calculation procedure are done. Inverter and PWM control were also implemented in the above simulation studies and the simulation based fine-tuned control parameters are used in the practical implementation of the motor. Also, the closed loop control performance of the motor is satisfactory. For a very high-power dense drive the thermal analysis is very critical. It is observed that the junction temperature is within the limits *i.e.* less than 85 degrees Celsius as per the datasheet. This ensures a robust and faultless operation of the drive while switching high currents. This work can be implemented to design higher power drives validating the performance in switching high currents and to design a thermally robust controller.

REFERENCES

[1] Andrea Cavagnino, Mario Lazzari, Francesco Profumo and Alberto Tenconi, "A Comparison between the Axial Flux and the Radial Flux Structures for PM Synchronous Motors", IEEE TRANSACTIONS ON INDUSTRY APPLICATIONS, VOL. 38, NO. 6, NOVEMBER/DECEMBER 2002.

[2] Amit N. Patel et.al, "Comparative Performance Analysis of Radial Flux and Dual Air-Gap Axial Flux Permanent Magnet Brushless DC Motors for Electric Vehicle Application", 2nd IEEE International Conference on Power Electronics, Intelligent Control and Energy Systems (ICPEICES - 2018).

[3] P. Rama Mohan et.al, "A Simple Generalized Pulse Width Modulation Algorithm for Vector Control based Voltage Source Inverter fed Induction Motor Drives", International Conference on Magnetics, Machines & Drives (AICERA-2014 ICMMD).

[4] F. Vijay Amirtha Raj, Dr. V. Kamatchi Kannan, "Analysis of Different Speed Control Techniques Using PMSM", International Journal of Innovative Research in Electrical, Electronics, Instrumentation and Control Engineering ISO 3297:2007 Certified Vol. 4, Issue 10, October 2016.

[5] Chung-Hui Lee, Hui-Seong Shin and Ki-Chan Kim (2022), Analysis of Interior Permanent Magnet Synchronous Motor according to Winding Method. IJEER 10(2), 207-213. DOI: 10.37391/IJEER.100227

[6] Uwe DROFENIK, Johann W. KOLAR, "A General Scheme for Calculating Switching- and Conduction-Losses of Power Semiconductors in Numerical Circuit Simulations of Power Electronic Systems", Power Electronic Systems Laboratory (PES), ETH Zurich ETH-Zentrum / ETL H13, CH-8092 Zurich, Switzerland.

[7] Geetha K, Sreenivasappa B V, "POWER LOSS CALCULATION FOR IGBT and SiC MOSFET", Journal of Xi'an University of Architecture & Technology, ISSN No : 1006-7930, Volume XII, Issue VIII, 2020, Pp.378-382.

[8] Sandhya Kulkarni and Archana Thosar (2022), Performance Analysis of Fault Tolerant Operation of PMSM using Direct Torque Control and Fuzzy Logic Control. IJEER 10(2), 297-307. DOI: 10.37391/IJEER.100240.

[9] Zhenyu Yu et.al, "Space-Vector PWM With TMS320C24x/F24x Using Hardware and Software Determined Switching Patterns", Digital Signal Processing Solutions, Application Report SPRA524, Texas Instruments.

[10] V. Sailaja, K. Nagabhushan Raju, "PID Controller Tuning using Ziegler-Nichols Method for Temperature control of Thermal Cycler", International Journal of Advanced Research in Electrical, Electronics and Instrumentation Engineering (A High Impact Factor, Monthly, Peer Reviewed Journal) Website: www.ijareeie.com Vol. 8, Issue 4, April 2019.

[11] Vasudeva Naidu Pudi, GVSSN Srirama Sarma, Srinivasa Rao Sura, Prasad Bolla and N Siva Mallikarjuna Rao (2021), Modelling of Electric Vehicle with PID Controller Transfer Function using GA and Model-Reduced Order DRA Algorithm. IJEER 9(4), 135-142. DOI: 10.37391/IJEER.090407

[12] Nicolaus Allu, Apriana Toding, "Tuning with Ziegler Nichols Method for Design PID Controller at Rotate Speed DC Motor", IOP Conf. Series: Materials Science and Engineering 846 (2020) 012046 IOP Publishing doi:10.1088/1757-899X/846/1/012046.

[13] M. Jiménez, J. Tapia, P. Lindh, L. Aarniovuori, A. Anttila and J. Pyrhönen, "Alternative Procedures for Thermal Design on Electric Machine," 2021 IEEE International Electric Machines & Drives Conference (IEMDC), 2021, pp. 1-6, doi: 10.1109/IEMDC47953.2021.9449555.

[14] Lipeng Tan et.al. "Heat Dissipation Characteristics of IGBT Module Based on Flow-Solid Coupling", Micromachines 2022, 13, 554. https://doi.org/10.3390/mi13040554.